BNL-105700-2014-TECH

BNL/SNS Technical Note No. 131;BNL-105700-2014-IR

Estimate of Dose and Residual Activity in the SNS Ring Collimation Straight

H. Ludewig

December 2003

Collider Accelerator Department

Brookhaven National Laboratory

U.S. Department of Energy

USDOE Office of Science (SC)

DISCLAIMER

Estimate of Dose and Residual Activity

in the SNS Ring Collimation Straight

BNL/SNS TECHNICAL NOTE

NO. 131

H. Ludewig, N. Simos, D. Davino*, S. Cousineau+, N. Catalan-Lasheras**, J. Brodowski, J. Touzzolo, C. Longo, B. Mullany, and D. Raparia
Brookhaven National; Laboratory, Upton, New York, 11973, USA.
*Univesita' del Sannio, Benevento, Italy.
+Oak Ridge National Laboratory, Oak Ridge, Tennessee. USA.
** CERN, 1211 Geneva 23, Switzerland.

December 30, 2003

COLLIDER-ACCELERATOR DEPARTMENT
BROOKHAVEN NATIONAL LABORATORY
UPTON, NEW YORK 11973

Estimate of Dose and Residual Activity in the SNS Ring Collimation Straight

H. Ludewig, N. Simos, D. Davino*, S. Cousineau+, N. Catalan-Lasheras**, J. Brodowski, J. Touzzolo, C. Longo, B. Mullany, and D. Raparia
Brookhaven National; Laboratory, Upton, New York, 11973, USA.
*Univesita' del Sannio, Benevento, Italy.
+Oak Ridge National Laboratory, Oak Ridge, Tennessee. USA.
** CERN, 1211 Geneva 23, Switzerland.

Abstract

The collimation system in the SNS ring includes a two-stage collimator consisting of a halo scraper and an appropriate fixed aperture collimator. This unit is placed between the first quadru-pole and the first doublet in the collimation straight section of the ring. The scraper is situated at the exact mid-point between these two magnets, and the fixed aperture collimator fills the space between the scraper and the doublet magnet. The scraper mechanism and collimator are mounted on a common plate, which is adjusted by three jacks. The entire structure is surrounded by an outer shield structure. The downstream dose to the doublet and the attached corrector magnet will be estimated for normal operating conditions. In addition, the activities of cooling water, tunnel air, and dose to cables will be estimated. The dose at the flange locations will be estimated following machine shutdown. In addition, the dose to cables, tunnel air, and the effectiveness of the moveable shields will be made. Finally, the implied dose to surroundings during the removal of an exposed collimator will be made.

Introduction

A two-stage halo cleaning system, consisting of a beam scraper and primary fixed aperture collimator is placed between the first quadru-pole and the first doublet in the collimation straight. Halo particles that are intercepted by the scrapers undergo sufficient Coulomb scattering to either deflect them directly into the primary collimator or one of the other collimators in the collimation straight. If the scattered particles are not intercepted on the first pass they will generally be intercepted within the next few circuits around the ring. The scraper is placed at the mid-point between these magnets, and the collimator is placed between the scraper and the doublet. The scrapers will be placed at approximately 140 pmm-mrad, and the fixed aperture of the collimator will be at approximately 300 pmm-mrad. The beam shape at this position is highly elliptical, and thus the beam tube of the collimator will be elliptical with y/2=48 mm, and x/2=79 mm, respectively. The length of the elliptical section of the collimator tube is 1.8 m, and the overall length including transition pieces and end shielding is 2.463 m. The secondary and tertiary fixed aperture collimators both have circular cross sections with a diameter of 62 mm.

All fluxes, and heat depositions were determined by the Monte Carlo code MCNPX [1]. The activation estimates were carried out using fluxes determined by MCNPX, nuclear data from the CINDER90 library [2], and transmutation determinations by a suitably modified version of the ORIGEN code [3]. The linkage between the various codes and data packages is shown in Fig. 1. The activation following machine shutdown was determined by using the gamma-ray source in each volume of interest as a source input in a photon transport calculation using MCNPX. The gamma-ray source as a function of energy is determined by the ORIGEN code, and is a function of the decay products in the cell at the time of interest (immediately following shutdown, or following a decay period).

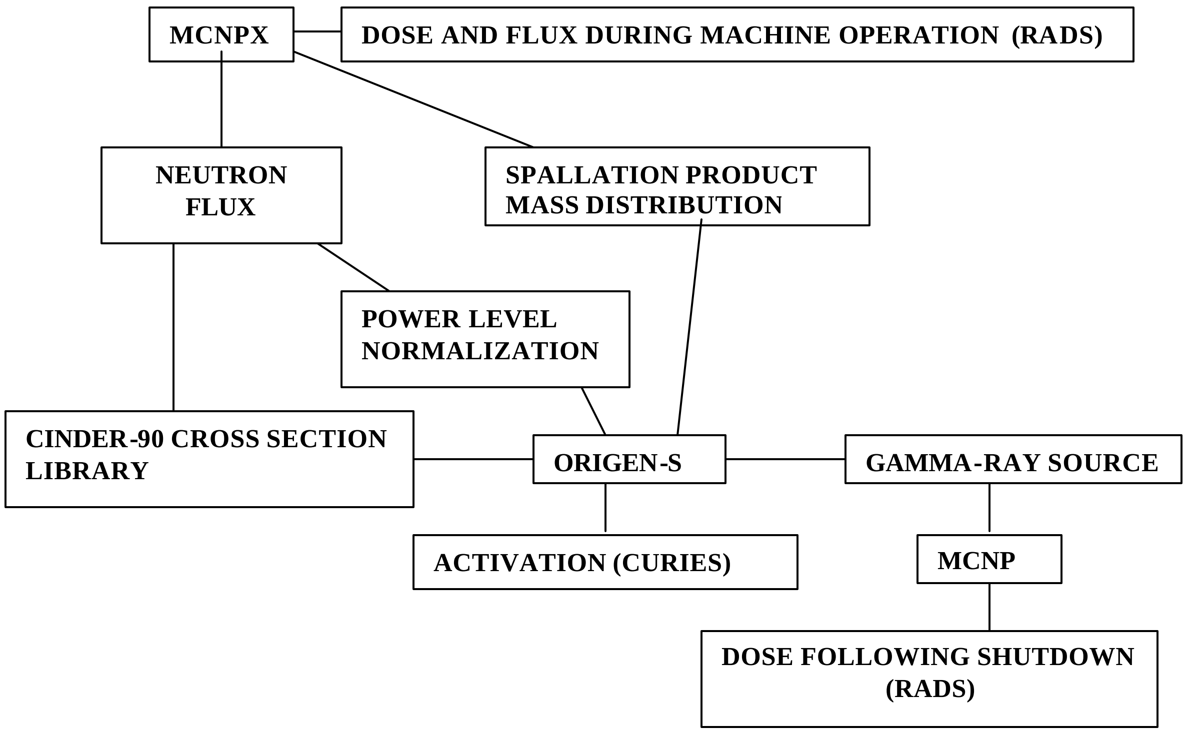

Fig. 1 – Linkage between codes and data packages used in determining dose and activation.

The fixed aperture collimator consists of a double walled tube manufactured of Inconel-718 [4], surrounded by a water-cooled bed of stainless steel spheres, which in turn is surrounded by a stainless steel shield. This entire configuration is contained in a pressure vessel. Cooling water flows through the particle bed of stainless steel spheres cooling both the spheres and the outer surface of the outer Inconel-718 collimator tube. The space between the inner and outer Inconel-718 tubes if filled with pressurized helium and a copper wire wrap, which enhances the heat transfer from the inner tube to the outer tube. The scraper mechanism and the collimator will be mounted on a common pedestal in order to ensure alignment, regardless of floor motion. Both components are enclosed in an outer iron shield that reduces dose to the tunnel environment during operation, and in particular reduces the dose to the scraper drive motors. In the downstream direction the magnet shielding is enhanced by a piece of stainless steel. Due to the proximity of the shield to the magnet non-magnetic material must be used in this location for the primary collimator. Secondary and tertiary collimators are sufficiently far removed from magnets that they can use iron as an outer shield material. The primary collimator, scraper mechanism, and the common mounting plate are shown in Fig. 2. The remaining fixed aperture collimators used in the HEBT, Ring, and the RTBT are similar to the primary collimator described above. The primary difference is that they have circular apertures (40 mm in the HEBT, 62 cm in the Ring, and 86 cm in the RTBT), and have slightly different overall lengths (297.2 cm in the Ring and RTBT, and 274.3 cm in the HEBT). They all have a bed of randomly packed stainless steel particles that are water cooled for absorbing the bulk of the primary beam halo. In addition the use of a particle bed makes it feasible to absorb the thermo-mechanically enhanced thermal stresses resulting from a full power beam loss on the collimators. The mechanical design is capable of absorbing at least two full power pulses. After this time the beam-interrupt system should terminate operation of the machine. Detailed descriptions can be found elsewhere [5-8].

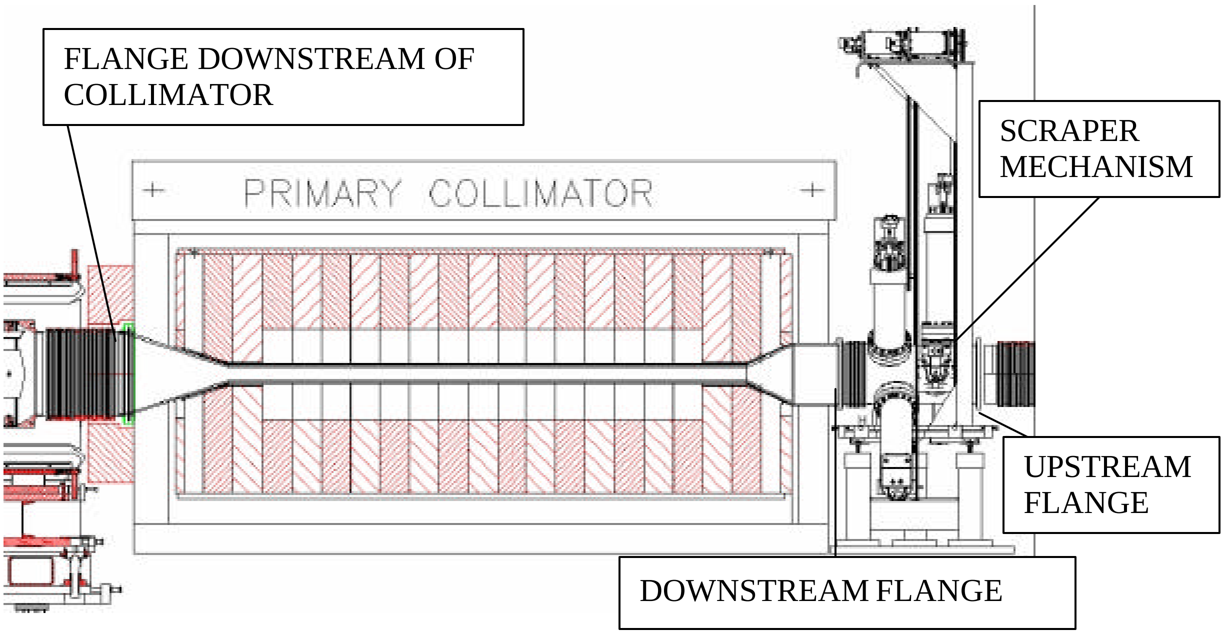

Fig. 2 – Beam Scraper and Fixed Aperture Primary Collimator

A detail view of the scraper mechanism in the direction of the proton beam, is shown on Fig. 3. Each of the scrapers consists of tantalum piece 0.5 cm thick in the direction of the beam, 1.0 cm high, and 5.0 cm wide. This piece is welded to a water-cooled copper block, which in turn is attached to a mechanism to allow motion in and out of the beam. The four tantalum scraper surfaces are visible inside the vacuum chamber. Each drive mechanism is attached to a drive motor by a chain that allows for precise motion of the scraping surface. Not shown in the figure are the flexible cooling water lines. However, each mechanism will have two lines for cooling water, which will be brought up to the top were they will be connected to an intermediate heat exchanger. An intermediate heat exchanger will be necessary, since the cooling water will become activated, and thus building service water will not be permissible as the primary cooling source. Limit switches will be integrated into the mechanism to limit the travel of the tantalum scrapers to the halo of the circulating beam. Interaction of the scraper with the full beam will prove to be damaging for the tantalum surface, and will eventually lead to failure. The machine protection system, which will be integrated with the loss monitors should limit this possible failure mode, since a significant neutron and gamma-ray source will result from direct interaction of the beam with the tantalum scrapers. The entire scraper mechanism and its frame are positioned on three precisely positioned pins, which in turn are fixed to a structure that is attached to the plate supporting the fixed aperture collimator. In this way the scraper can be exchanged without removing the collimator, and the replacement scraper can be put in place remotely by lowering it on to the three pin locations. Alignment with the collimator is maintained in this manner, making it easier to attach the flange between the scraper and collimator.

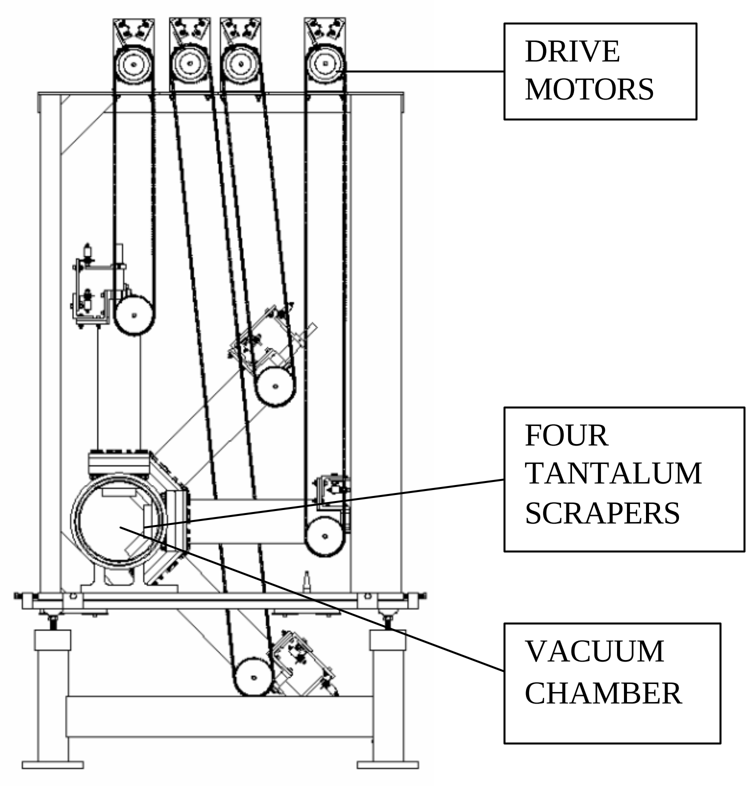

Fig. 3 – Beam Scraper Mechanism

The loss distribution of scattered particles along the inner surface of the primary collimator tube is required to determine the resulting doses to surrounding components. The distribution assumed in this study, as a percentage of the particles lost on the tube surface, is shown on Fig. 4. It is seen that there is a relatively high loss (~ 10 %) at the entrance to the collimator, and the bulk of the collimator has a relatively constant loss of ~ 4.4 %. This loss profile is used as input to the Monte Carlo code MCNPX, which determines the fluxes of secondary particles, resulting

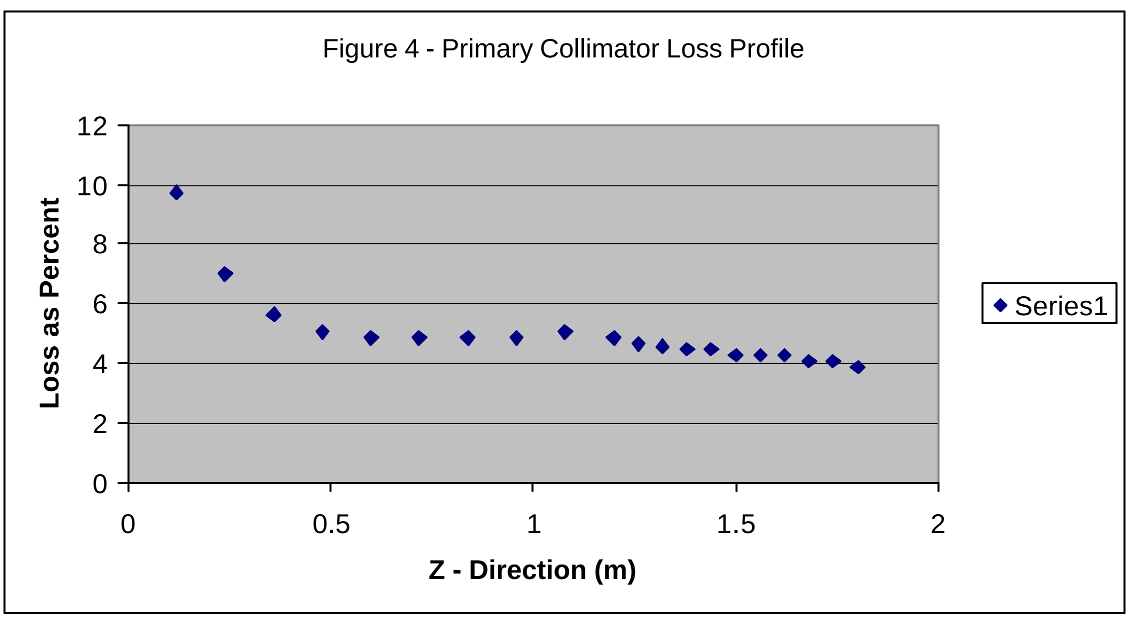

from the shower created by the interaction of primary particles with the collimator mass.

Results

In these sections we will discuss the estimated results of doses and residual activation in the vicinity of flange areas on either side of the primary collimator and scrapers, to the scraper drive motors, the downstream magnets, cables, and tunnel air. In addition, implied doses due to removal of a collimator following machine shutdown, will be discussed. The loss fraction under normal operating conditions in the ring is assumed to be 0.001 of the circulating beam, of this fraction 5 % is lost on the scrapers, and 30 % is lost on the inner surface of the primary collimator. Thus, the loss fraction on the scrapers is 0.00005, and the loss fraction on the collimator is 0.0003. Implications of loosing the entire beam on the collimator will also be discussed. Furthermore, the assumption will be made that the machine is operating at 2 MW for one year (defined as 250 days, or 2.16×10^7 seconds) unless otherwise stated.

Doses to components around the primary collimator and scraper

During normal operation of the machine the dose for one year is given below at the flanges (both upstream and downstream of the collimator and scraper), and the downstream magnet.

Table 1 – Dose to Flanges while Machine is operating
(rad/yr)

Location Description	Collimator dose	Scraper dose	Total dose
Flange upstream of Scraper	1.20(5)*	1.71(6)	1.83(6)
Flange downstream of Scraper	4.87(5)	7.54(6)	8.03(6)
Flange downstream of Collimator	2.47(7)	~	2.47(7)
Magnet downstream Of Collimator	4.83(7)	~	4.83(7)

*1.20(5) = 1.20×10^5

The above dose to the flanges requires that they be radiation hardened against neutron, proton and gamma-ray radiation. The magnet placed downstream of the collimator requires that the insulation be as radiation hardened as possible. Assuming that Kapton will be used as the magnet insulating material, and assuming that its life is approximately 2(9) rads, then the magnet life under normal conditions should be ~ 40 years. Addition of a 10 cm thick stainless steel shield piece between the magnet and the collimator reduces the dose by approximately 10 %, thus increasing the life by the same amount. Assuming that the entire ring loss fraction takes place in the primary collimator, or the overall ring loss increases by approximately a factor of three the dose to the magnet increases to 1.6(8) rads, and the implied life of the magnets would be reduced to ~ 12 years. Higher losses or a lower radiation damage resistance limit for the Kapton insulation, would both reduce the magnet life in proportion to the change.

Following machine shutdown the level of radiation at the flanges is of interest, since they may have to be accessed for maintenance purposes. An estimate was made of the potential dose at the flange locations following a 180 day period of operation at 2 MW average power, and with a loss fraction of 35 % of the total ring loss on the scraper-collimator assembly (5 % on the scraper, 30 % on the collimator). The estimated dose at the four locations described above, immediately following shutdown, are given below.

Table 2 – Dose to Flanges following machine shutdown

Location Description	Dose (mrad/hr)
Flange upstream of Scraper	84
Flange downstream of Scraper	5025
Flange downstream of Collimator	490
Magnet downstream of Collimator	790

It is seen that immediately following machine shutdown the dose to the flange located between the scraper and the collimator is quite high, and a decay period would be advisable before maintenance activities are carried out. If the loss in the ring were concentrated at the primary collimator the dose values would increase by approximately a factor of three.

An estimate of the reduction in the above values following a decay period can be obtained by determining the reduction in activation for both the tantalum scrapers and the stainless steel collimator components. The decay of these components is given below, and is seen to be quite different. The normalized activation decay for representative volumes of these two components is given below.

Table 3 – Decay of Activation of Tantalum and Stainless steel following machine shutdown

Material	Time following machine shutdown				
	0.0	4 hours	1 day	7 days	30 days
Stainless steel	1.0	0.776	0.677	0.537	0.328
Tantalum	1.0	0.462	0.284	0.125	0.061

These estimates indicate that the collimator will decay at a much slower rate than the scrapers. Thus, those locations at which the scraper dose is a major contributor (flange upstream of the scraper) will decay faster than the other locations. However, if a decay period of approximately one day is allowed in the maintenance schedule, then the dose should be reduced by ~ 50 %. Following one day the reduction in the dose is expected to be more modest. Finally, if the losses in the ring are concentrated at the primary collimator these doses would increase by a factor of three.

The dose to the scraper drive motors while the machine is operating is of concern, since eventually a high enough dose will compromise the motor insulation. Estimates of dose at the motor location were made, assuming that 5 % of the loss occurs on the scrapers, and an iron shield was inserted between the scraper mechanism and the motors. Two values for the shield thickness were assumed, and the corresponding doses estimated. Results are given below, and indicate that an iron shield of nominal thickness implies an acceptable motor life, assuming the same radiation damage resistance as that given above for the magnets. If the loss increases to the maximum ring loss the dose values increase by a factor of 20, and the condition of the drive motors should be monitored.

Table 4 – Dose to scraper drive motors

Iron shield thickness (cm)	Dose (rad/yr)
15	1.1(5)
30	5.5(4)

The iron shield will be designed in such a manner that it allows passages for the scraper drive chains, and cooling water lines.

Collimator cooling water residual activity

An estimate was made of the residual activity in the collimator and scraper cooling water immediately after shutdown and following 4 hours of decay time. These estimates assume that the ring loss is confined to the primary collimator. The scraper activity is estimated by scaling off the values obtained for the collimator. The machine is assumed to operate at 2MW for a period of 180 days, and the loss fraction is 0.001 of the circulating beam. Immediately following shutdown, the activity is dominated by the short half-lived isotopes ^{15}O, ^{16}N, ^{11}C, and ^{12}B. After a 4 hour decay period the dominant contributors to the activity are ^{7}Be, and ^{14}C. Note is also taken of ^{3}H, although its total activity is low, and its contribution to the overall activity marginal. The activity of the collimator water following a 4 hour decay period is given in table 5.

Table 5 – Residual activity of Collimator cooling water 4 hours after machine shutdown (Curies)

Isotope	Activity
Tritium (^{3}H)	2.6(-8)
Beryllium (^{7}Be)	6.1(-2)
Carbon (^{14}C)	2.2(-5)

Scraper cooling water activity is a fraction of the above collimator cooling water activity. A direct scaling of the activity by the loss fraction would result in a reduction of the above values by a factor of six. However, this reduction is optimistic, since the collimator water is exposed to the high-energy proton and neutron beam, while in the scraper the geometric arrangement essentially precludes the interaction of the very high-energy particles from seeing the cooling water. Beryllium is created as a spallation product off the oxygen nuclei in the water following interaction with the very high-energy particles. This interaction is greatly reduced because the very high-energy particles are created in a forward facing cone and thus largely by-pass the scraper water. It is to be expected that, under the assumptions stated above, the ^{7}Be activity will be reduced by at least an order of magnitude from the above mentioned value and the tritium and ^{14}C activity will be reduced by approximately a factor of six. The primary cooling circuit, and the intermediate heat exchanger should be embedded in an appropriate shield, since the presence of ^{7}Be implies a source of approximately 0.5 MeV gamma-rays.

Dose to cables in collimation straight

A cable tray was assumed to be located along the wall of the ring, at an elevation of 1 m above the centerline of the beam. The maximum dose to cables was found to be opposite the primary collimator/scraper location. It was assumed that the entire loss fraction at the primary collimator is ~ 35 % of the ring total ring loss (0.001 of circulating beam). Under these conditions it was found that the maximum dose to cable insulation will be ~ 250 rads/hour during machine operation. Assuming a dose limit of approximately $1x10^{8}$ rads for cable material implies a life of ~ 80 years. This value will vary depending on loss fraction, radiation hardness of the cable insulation, and final position of the cable tray.

Tunnel air activation

An estimate was made of the tunnel air activation in the vicinity of the primary collimator-scraper assembly. The atmosphere included oxygen, nitrogen, hydrogen, and argon. Immediately following shutdown of the machine the activation was dominated by ^{13}N, ^{37}Ar, ^{39}Cl, and ^{16}N. Following four hours of decay time the dominant activity is due to ^{14}C. At shutdown the activity is ~ 0.06445 Curies, following the four hour decay time the activity drops to 0.00426 Curies, and then decreases gradually as the ^{14}C decays. These estimates were made assuming no atmospheric motion. In a real situation, the air would likely be circulated and vented following an appropriate holdup period to ensure that the short-lived isotopes have decayed. In this manner the buildup of activity can be controlled.

Dose between primary and secondary collimators

An estimate of dose between the primary collimator, the down-stream doublet magnet, and the secondary collimator was made following machine shutdown and waiting for a decay period of four hours. The machine was assumed to operate at 2 MW for 180 days before the shutdown. In these calculations, unlike those reported on above, the tunnel walls were also included, thus any reflections off the walls are included in the dose. The configuration considered in this estimate is shown in Fig. 5, which shows the upstream end of the primary collimator, the magnets, and the downstream end of the secondary collimator. In addition, the moveable lead shielding is shown placed axially along the vacuum chamber. The dose was estimated by placing spheres of water at the locations shown in the Fig 5. And determining the energy deposited in the sphere from the decay gamma-rays. This method results in the determination of the energy deposited in MeV/gm-p^{+}, which is converted to rads/s by multiplication by the proton current and$1.602x1.0^{-8}$. The results obtained for the dose estimates are given in table 6.

Table 6 – Shielded doses between the primary and secondary collimators following machine shutdown behind moveable shield
(mrads/hr)

Location	Dose

Next to primary collimator (r ~ 0.5 m)	300
Next to primary collimator (r ~ 1.0 m)	180
Opposite first quadru-pole (r ~ 0.5 m)	80
Opposite first quadru-pole (r ~ 1.0 m)	60
Opposite second quadru-pole (r ~ 0.5 m)	60
Opposite second quadru-pole (r ~ 1.0 m)	80
Next to secondary collimator (r ~ 0.5 m)	400
Next to secondary collimator (r ~ 1.0 m)	250

These values are consistent with those reported in table 2, despite the fact that different primary beam loss profiles were assumed in the two calculations. The dose closest to the collimator faces is due primarily to the residual activity of the outer collimator shielding. The dose furthest from the collimators, and behind the moveable shield is not entirely zero, primarily due to reflections off the tunnel walls. It is thus essentially impossible to reduce the dose to essentially zero, since the accelerator components will always act as sources, and the walls as reflectors of gamma-rays.

Effect of magnetic field on dose to doublets

An estimate of the dose to the quadru-pole magnets, including the effect of the doublet magnetic field on the secondary particles created by the halo (protons in this case), will be made in this section. The doublet magnet is located between the primary collimator and scraper assembly and the secondary collimator located downstream of the doublet. The dose estimates were made using the MCNPX code, with an appropriate modification that allows tracking of charged particles through magnetic fields [9,10]. The magnetic field profiles were generated by the COSY INFINITY code [11]. The pre-generated data is in a form of a map, which is assigned to each magnetic cell in the MCNPX input file. The dose to the selected components will be determined in the same manner as described above. The doublet and corrector magnets are located between the back face of the primary collimator and the front face of the secondary collimator. The two quadru-pole magnets making up the doublet are 0.7 m and 0.55 m in length, and have magnetic fields of 0.5 T and 0.55 T respectively.

In order to understand the effect of the magnetic fields on the secondary particles created by the halo, the beam pipe was divided into eight azymuthal intervals and the proton flux in each interval was determined with and without the field on. In addition, the dose to the quadru-pole magnet windings was determined with and without the magnetic field. The axial locations along the beam line of the cross sections of interest are at the exit of the primary collimator, between the quadru-poles of the doublet magnet, and the entrance to the secondary collimator. It is seen that with the magnetic field off, the azymuthal beam profile along the axial direction does not vary significantly from location to location, and it essentially reflects the scraped profile. That is, it is high over the azymuthal interval from 135° - 270°, and low 0° - 90° and 315° - 360°. However, with the magnetic fields turned on the profile varies quit significantly. It is seen that between the magnets the peak in the distribution is from 90° - 135°, and 225° - 270°, with minor peaks from 45° - 90° and 270° - 315°. Finally at the location before the secondary collimator the peaks are not as high, particles having been lost before the collimator, and the peak is broader and shifted to the interval 135° - 225°. The production of secondary particles increases following

inclusion of the magnetic field, since the deflected halo creates secondary particles when interacting with the magnet pole pieces.
Dose estimates were carried out assuming the machine operates at 1.5 MW, with a loss fraction of 0.001 on the scrapers and the front face of the collimator. The results are given in table 7, below. The results are for two faces of the quadru-pole magnet windings. Face number 1 is at 90° to face number 2. The remaining two faces are symmetrical to these two faces.

Table 7 – Dose with and without magnetic field of the doublet included (mrad/s)

Magnet/ face number	Without magnetic field	With magnetic field
First Quadru-pole/ face 1	277	309
First Quadru-pole/ face 2	196	533
Second Quadru-pole/ face 1	1577	711
Second Quadru-pole/ face 2	2328	1591

It is seen that the inclusion of the magnetic field due to the doublet increases the dose to the first magnet but decreases it to the second magnet. The overall conclusion regarding expected magnet insulation life still applies, but the importance of including either magnetic or electric fields in the trajectories of secondary charged particles and their effect on the dose, or heating, is evident.

Dose in the vicinity of a partially or unshielded collimator

In the event that a collimator should be moved, following machine operation at 2 MW for 180 days, and shutdown for four hours, the doses in the vicinity of the collimator will vary with position and the assumed loss pattern. In this study it was assumed that the loss takes place primarily at the entrance of the collimator tube, and that the loss fraction is 0.001 of the full beam intensity. The expected dose around a collimator with all the shielding removed. However, this case is not possible in practice since the inner box is welded to the collimator in the current design, and so there would always be some shielding available. Results and the conceptual ideas outlined here still bear discussing here, since they apply to the currently designed configuration. The highest dose (~ 10,000 rads/hr) occurs along the centerline inside the collimator at the location of the beam loss. This dose drops off with distance along the beam line until it is 13.5 rads/hr at a distance of 2 m. At a radius of 47.5 cm the dose on the surface of the collimator is 19.2 rads/hr, which then increases to 42.5 rads/hr at an axial distance of 1 m, and then decreases to 13.8 rads/hr at a distance of 2 m. Increasing the radial distance to 75.0 cm and moving axially away from the plane of the collimator face shows that the dose increases from 4.6 rads/hr to 30.3 rads/hr and then decreases to 12.6 rads/hr.
This dose pattern indicates that it is "flash-light" like in structure, with a beam of gamma-rays coming out at the end. At a distance beyond ~ 2 m axially downstream the dose is approximately constant with a flat peak along the centerline. The behavior described above also applies to the other end of the collimator as well . However, due to the assumed loss pattern, which concentrates the loss at opposite end, the values are lower by approximately two orders of magnitude. Finally, the results for a single collimator surrounded by the inner shield box are shown on Fig. 6. It is seen that the same behavior is exhibited as described above. The values are

lower by approximately a factor of two, along the centerline, and larger reductions are evident at larger values of the radius. This reduction in dose is due to the shield attenuating gamma-rays (other than those starting in the vacuum chamber) and thus reducing their contribution to dose values. At the outer radius if the collimator inner shield the dose is ~ 0.01 rads/hr. At the axial distance of ~ 2m the dose has dropped to ~ 5 rads/hr compared to the above unshielded case of ~ 12 rads/hr.

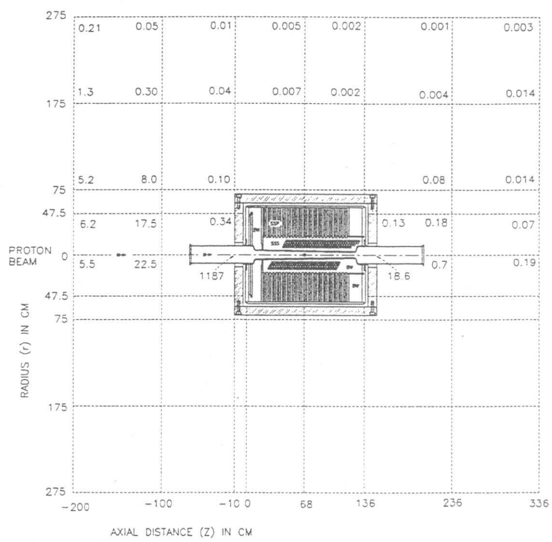

FIG 8 – DOSE IN REM/HOUR AROUND COLLIMATOR
WITH 10 CM THICK INTERNAL SHIELD

Dose around HEBT momentum dump

The shielding requirements, and thus the implied doses at the HEBT momentum "dump" is of interest, since there might be a requirement to route cable across the top of the structure. In order to estimate the dose as a function of lateral concrete thickness a model of the dump was constructed. The actual dump consists of a rectangular shaped water cooled stainless steel particle bed 30 cm x 30 cm x 100 cm. It had a water-cooled window at one end, and wheels for installation at the other end. The dump is surrounded by an iron inner shield 58 cm thick on all sides. The outer shield consists of concrete, which is 80 cm thick at the inlet, and 120 cm thick at the back end, and of variable thickness on the lateral sides. The thickness range considered here is 50 cm – 100 cm. Values of the dose while the machine is operating at 2 MW with a loss fraction of 0.001 at the front, back and top of the dump plus shield assembly are given in table 7.

Table 7 – Dose at various positions around the HEBT momentum dump
(rads/s)

Lateral concrete thickness	Front	Top	Back
50 cm	0.0113	0.059	0.0047
75 cm	0.0113	0.0194	0.0047
100 cm	0.0113	0.0074	0.0047

The dose corresponding to the case with a 50 cm thick concrete layer is similar to the dose estimated for the high loss area in the vicinity of the primary collimator. It would thus be prudent to increase the concrete thickness to approximately 100 cm, in order to ensure no radiation damage induced problems with the cables following years of machine operation.

Conclusions

The following conclusions can be drawn from this study:

1) The loss profile along the fixed aperture collimator is biased to the upstream end, and thus affects the flange between it and the beam scraper the most,
2) Dose estimates based on the current loss profile and fraction will require the exchange of the downstream magnets at least once during the life of the machine,
3) Dose to the scraper drive motors is likely to be low enough to ensure that they will operate for the machine life,
4) The intermediate heat exchanger for the collimator and the scraper cooling water will require a shielded pipe to reduce the intensity of the gamma-ray from the Be-7 decay.
5) Maintenance work on the flanges will best be carried out following a decay period of at least one day to one week, in order to reduce the dose to the workers.
6) Doses to cables in the collimation straight section and in the vicinity of the HEBT momentum dump should be low enough to allow operation for the life

of the machine. However, if the losses increase beyond those assumed in this study cable failure cannot be ruled out.

7) Long-term tunnel air activation is dominated by ^{14}C, which can be mitigated by a ventilation system.
8) In the event that a collimator needs to be removed following a long period of operation, care should be taken to shield the gamma-ray shine from each end of the opened vacuum chamber. A custom made lead plug might be necessary.
9) The presence of a magnetic field interacts with the secondary particles created by the halo particles to increase the dose to magnet components. Future dose estimates of operating machines should include both magnetic and electric fields.

References

[1] *MCNPX Users Manual-Version 2.1.5*, L.S. Waters, ed., Los Alamos National Laboratory, Los Alamos, NM. TPO-E83-G-UG-X-00001. (1999)

[2] W.B. Wilson, "Accelerator Transmutation Studies at Los Alamos with LAHET, MCNP, and CINDER-90", Los Alamos National Laboratory, Los Alamos, NM. LA-UR-93-3080 (1993).

[3] A.G. Croff, ""ORIGEN2 – A revised and updated version of the Oak Ridge isotope generation and depletion code", Oak Ridge National Laboratory, Oak Ridge, TN. (1977).

[4] W. Sommer, R. Werbeck, S. Maloy, M. Borden, and R. Brown' "Materials selection and qualification processes at a high-power spallation neutron source", Materials Characterization, 43, 97 – 123. (1999).

[5] H. Ludewig, N. Simos, J. Walker, P. Thieberger, A. Aronson, J. Wei, and M Todosow,"Collimation system for the SNS Ring",PAC, New York City, [1999]

[6] H. Ludewig, N. Simos, N. Catalan-Lasheras,"Preliminary estimates of dose and residual activity of selected components in the ring collimation straight of the SNS",EPAC, Vienna, [2000]

[7] N. Simos, H. Ludewig, N. Catalan-Lasheras, J. Brodowski, and J. Wei," Thermo-mechanical response of the halo intercepts interacting with the SNS proton beam",PAC, Chicago, [2001]

[8] N. Simos, H. Ludewig, N. Catalan-Lasheras, and S. Crivello, "Double-walled collimator design of the SNS project",PAC, Chicago, [2001]

[9] H. Ludewig, A. Mallen, N. Catalan-Lasheras, N. Simos, J. Wei, and M. Todosow,"Effect of magnetic fields on the dose estimates due to beam halo loss in the Ring collimation straight of the SNS",PAC, Chicago, [2001]

[10] J. Favorite et al.,Trans. Am. Nuc. Soc., Vol. 81, 1999.

[11] M. Berz, "COSY INFINITY Users manual", 1998.